Materials Chemistry and Physics 246 (2020) 122828

Contents lists available at ScienceDirect

Materials Chemistry and Physics

journal homepage: www.elsevier.com/locate/matchemphys

Importance of the electrolyte cation on the non-covalent interactions in the electrooxidation of 1-heptanol on gold in 0.1 M alkali metal hydroxides

M. Soledad Ureta-Zañartu [a,*], Ana María Méndez-Torres [a,1], Francisco Fernández [a], Jacqueline Ilabaca [a], Carolina Mascayano [a], Claudio Gutiérrez [b]

[a] Facultad de Química y Biología, Universidad de Santiago de Chile, Casilla 40, Correo 33, Santiago, Chile
[b] Instituto de Química Física "Rocasolano", CSIC, C. Serrano, 119, 28006, Madrid, Spain

HIGHLIGHTS

- Dependence of the hydration of the OH group of 1-heptanol in 0.1 M alkaline hydroxides on the of cation nature.
- Dependence of the 1-heptanol oxidation rate on gold in 0.1 M MOH on the nature of the electrolyte cation.
- 1-heptanol electrooxidation rate on gold in 0.1 M alkaline hydroxides on the hydration of the alcoholic OH group.
- 1-heptanol electrooxidation rates on gold measured by cyclic voltammetry and electrochemical impedance spectroscopy.

GRAPHICAL ABSTRACT

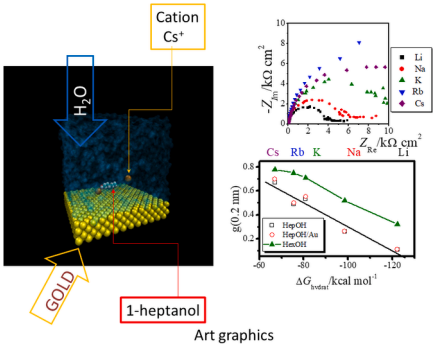

ARTICLE INFO

Keywords:
Non-covalent interactions
Hydration
Alcohol electrooxidation
Alkali metal hydroxides

ABSTRACT

In order to determine the possible non-covalent influence of the alkali metal cation on the electrooxidation of 1-heptanol on gold in alkali metal hydroxides, 0.1 M MOH solutions, where M = Li, Na, K, Rb, and Cs, have been used. The charge-transfer resistance, determined by Electrochemical Impedance Spectroscopy, of heptanol oxidation at a fixed potential increased monotonically by a factor of 4 from LiOH to RbOH, that is, the heptanol oxidation current decreased. Since the degree of hydration of the OH group of the alcohol, as estimated by Molecular Dynamics Simulation, increased by a factor of 5 from LiOH to RbOH, it can be concluded that the decrease of the heptanol oxidation current from LiOH to RbOH is due to an increasing hydration of the heptanol OH group, which would hinder its access to the electrode surface. This result is in line with the previous finding [M.S. Ureta-Zañartu, C. Mascayano, C. Gutiérrez, doi:10.1016/j.electacta.2015.02.230] that the increase of the alcohol oxidation current at a fixed potential of linear saturated aliphatic alcohols from C1 to C7 on gold, both in a pH 11 buffer and in 0.1 M NaOH, increased with increasing chain length, that is, with decreasing hydration (because of the increasing hydrophobicity) of the alcoholic OH group.

* Corresponding author.
E-mail address: soledad.ureta@usach.cl (M.S. Ureta-Zañartu).
[1] Facultad de Química y Farmacia, Universidad de Chile.

https://doi.org/10.1016/j.matchemphys.2020.122828
Received 26 August 2019; Received in revised form 16 December 2019; Accepted 15 February 2020
Available online 17 February 2020

1. Introduction

Non-covalent interactions have become an active research field. So, Strmcnik et al. [1] claimed that non-covalent interactions must be considered in the oxidation of methanol on platinum in alkali metal hydroxides. According to them, non-covalent interactions between hydrated alkali metal cations $M^+(H_2O)_x$ and adsorbed OH (OH_{ad}) species, generating $OH_{ad}^-M^+(H_2O)_x$ clusters, increase in the same order as the hydration energies of the corresponding cations (Li(+) ≫ Na(+) > K(+) > Cs(+)), and these clusters block the platinum active sites.

Recently, Nakamura et al. [2] reported that up to 1.2 V *vs* RHE the CVs of Au(111) in 0.1 M LiOH and 0.1 M CsOH fully coincided. The same occurred in the presence of 2.5 M methanol, and also in the presence of 0.2 M ethanol.

Already in 1986 Adzic and Avramov-Ivic [3] found by CV that in 0.1 M NaOH the onset potential of oxidation of ethylene glycol on the three basal planes of Au coincided with the onset potential of AuOH formation in base electrolyte, which critically depended on the crystallographic orientation, increasing in the order Au(100) < Au(110) < Au(111). (They assumed that the low-current plateau that preceded the main peak of Au oxidation corresponded to AuOH). Any non-covalent interaction of the alcohol oxidation should affect how the OH group of the alcohol interacts with the OH group on the surface of Au.

In a previous work [4] we found that the longer the chain length, from C1 to C7, of linear saturated aliphatic alcohols on gold, both in a pH 11 buffer and in 0.1 M NaOH, the lower was the onset potential for alcohol oxidation, that is, the easier was the oxidation of the alcohol. We attributed this trend to the increasing hydrophobicity of the alcohol with increasing chain length, which would decrease the degree of hydration of the OH group of the alcohol, facilitating its access to the electrode surface. This hypothesis was supported by Molecular Dynamics Simulations [4]. This previous work has led us to study if the nature of the cation in 0.1 M MOH electrolytes, where M = Li, Na, K, Rb and Cs, could non-covalently affect the degree of hydration of the OH group of 1-heptanol, and if this, in turn, affected its electrooxidation on polycrystalline gold. For this purpose, cyclic voltammetry (CV), electrochemical impedance spectroscopy (EIS), electrochemical quartz crystal microbalance (EQCM), and Molecular Dynamics Simulation (MDS), were used. We had to resort to the measurement of the charge-transfer resistance by EIS for determining the activity for 1-heptanol electrooxidation in the different electrolytes, since these differences were very small. Actually, even the electrochemical rate constant can be determined by EIS [5].

2. Experimental

2.1. Reagents

NaOH (pellets, 99%, Merck), KOH (pellets, >85%, Fluka) were used. LiOH (granules 98%), RbOH (50 wt% aqueous solution, 99.9% trace metals basis), CsOH (50 wt% aqueous solution, 99.9% trace metals basis) and analytical grade 1-heptanol were from Sigma Aldrich. The solutions were freshly prepared in twice distilled water, and the experiments were carried out at room temperature under a nitrogen atmosphere.

2.2. Electrochemical equipment

Two electrochemical work stations, CHInstrument 660c and Autolab PGstat 128 N, with EQCM and FRA modules, were used. The working electrodes were: gold discs (at least a different one for each cation), 0.2 cm in diameter, from CHInstruments, and an Au/quartz crystal electrode (Au/QCE, 10 MHz AT-cut quartz crystals with a thin film of gold (0.25 cm^2 geometrical area, and 0.24 cm^2 resonant area) from Elchema. The electrodes were cleaned by at least 5 repetitive potential cycles in the support electrolyte. A gold counter electrode of high area (ca 1.9 cm^2) and an Ag/AgCl/3 M KCl (+0.210 V *vs.* SHE) reference electrode were used. The latter was located in a vertical tube containing support electrolyte, and with a closed glass stopcock to avoid chloride diffusion into the cell. (In the EQCM experiments a $Hg/Hg_2SO_4/K_2SO_{4(sat)}$, (+0.65 V *vs* SHE) reference electrode was used, in order to decrease the electrical noise). Current densities (*j*) were referred to the geometrical area (0.031 cm^2 for the CHI disk, 0.25 cm^2 for the Au/QCE). The roughness factors of the gold discs and of the Au/QCE electrodes were 2.5 ± 0.3 and 1.33 ± 0.2, respectively, taking a value of 400 μC cm^{-2} for the reduction of an AuO monolayer in acidic media [6].

Electrochemical impedance spectroscopy (EIS) at a constant potential was carried out at 0.10 V *vs* Ag/AgCl using a sinusoidal modulation of 5 mV in a frequency range of 10 kHz to 10 mHz, with a logarithmic decrease of frequency, with 10 points per decade. The analysis of the impedance spectra was performed with the NOVA 2.1 software, that includes a Kramers-Kronig transformation (KKt).

2.3. Molecular Dynamics Simulation (MDS)

The alcohol was modelled with the Gaussian View software. The ChelpG charges for all atoms were assigned using the B3LYP/6-31G** basis set in Gaussian 09 software [7]. The hydroxides of Cs, Na, K, Rb and Li at a 0.1 M concentration in a water box (see below) were added by Chimera software [8] and the complete ensembles of the system were built in Visual Molecular Dynamics (VMD).

The Molecular Dynamics simulations were performed using NAMD 2.6 [9] with the Charmm 33 b1 force field [10]. Four Au{111} layers were built with the inorganic builder module in VMD, one 1-heptanol molecule was placed on top of the Au, and finally a 50 x 50 × 50 $Å^3$ water box with about 3895 water molecules was added. We applied a cutoff of 10 Å for non-bonded interactions and performed 250 ps of water equilibration, 10000 steps of minimization and 50 ps of heating from 0 K up to 310 K before each Molecular Dynamics simulation, which was 10 ns long. The temperature was kept constant using Langevin's method (300 K) and all the system was neutralized. All graphical analyses (Radial Distribution Function, RDF) were performed with the VMD software [11] using a correction parameter of monomer, added into the Charmm Force Field with the CcpNmr ACPYPE web server [12].

3. Results and discussion

The Au disc electrodes (CHI) were characterized by cyclic voltammetry in 0.5 M H_2SO_4 at 0.1 V s^{-1}. The first CVs at 0.01 V s^{-1} of the stabilized gold disc electrodes in 0.1 M MOH with M = Li, Na, K, Rb and Cs (Fig. 1A) show the characteristic region of surface oxide formation (peak 1a) and its reduction (peak 1c). The plots of the onset potentials for gold oxide formation, taken to be as those at which the current density was 10 and 15 μA cm^{-2}, at 10 and 20 mV s^{-1}, respectively, *vs* the Gibbs hydration energy (ΔG_{hydrat}) of the cations [13] are given in Fig. 1B. While at 0.01 V s^{-1} the onset potential barely increased with increasing hydration energy of the cation, at 0.02 V s^{-1} the opposite behaviour was clearly apparent, and so no correlation between the two magnitudes could be established.

In the EQCM experiments, the cell with the previously cleaned electrode was refilled with fresh electrolyte and deaerated with N_2 for 30 min at open circuit. The potential was then held at −0.60 V vs Hg/Hg_2SO_4 (−0.16 V vs Ag/AgCl) for 1 min (with N_2 bubbling during the first 30 s, after which the mass decreased abruptly), and then a CV at 0.02 V s^{-1} between −0.60 V and ~0.25 V vs Hg/Hg_2SO_4 (−0.16 and~0.69 V *vs* Ag/Ag/Cl) was started. The mass/time curves in Fig. 2A have been overlapped at the minimum mass observed upon stopping the nitrogen bubbling. The thin lines in Fig. 2A correspond to the mass change during the CV.

The formation of a monolayer of AuO, taking Trasatti's value of 400 μC cm^{-2} [6], would produce a mass increase of 30.9 ng cm^{-2}, which multiplied by the roughness factor, 1.33, would yield a mass increase of

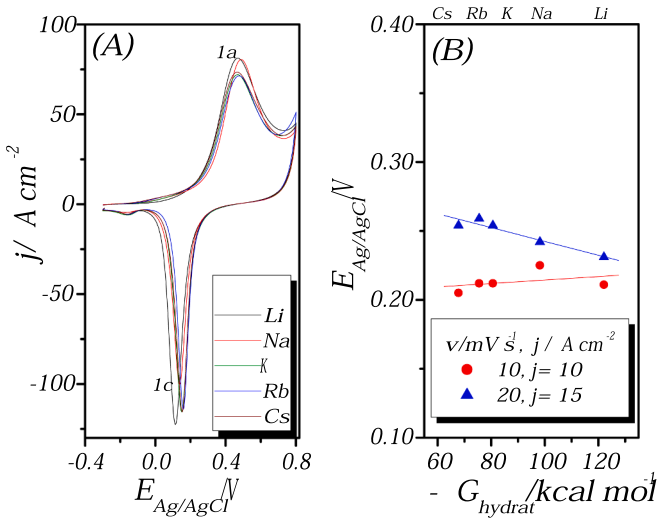

Fig. 1. (A)Cyclic voltammograms at 0.02 V s^{-1} of a gold disc electrode in 0.1 M MOH (M as in the inset). (B) Plot of the onset potentials of peaks 1a and 1c vs the Gibbs hydration energy of the respective cation. Closed and open symbols correspond to CVs carried out at 0.02 and 0.01 V s^{-1}, respectively.

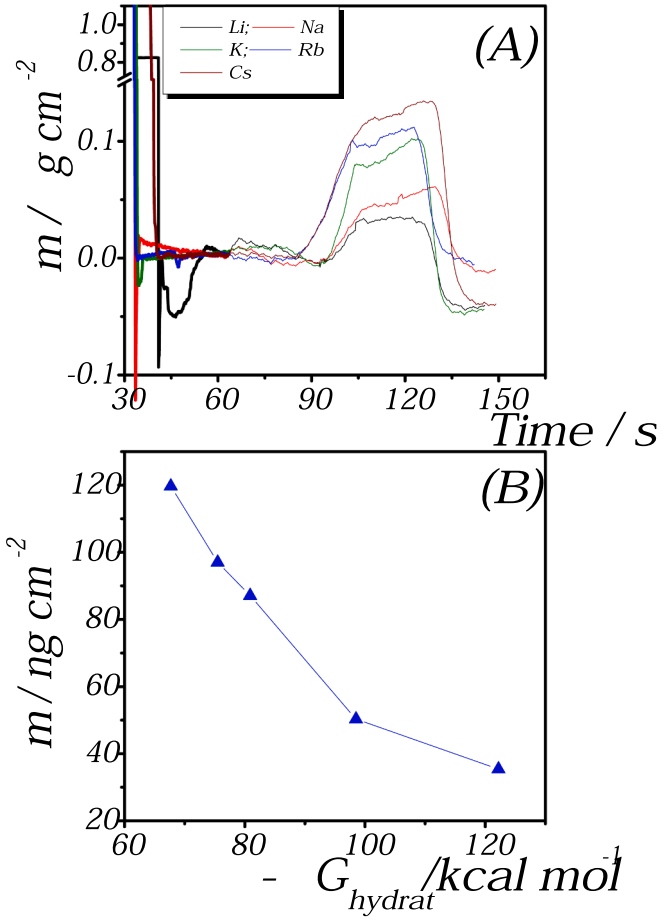

Fig. 2. EQCM study of the oxidation of a gold disc electrode in 0.1 M MOH. A: mass change during a CV at 0.02 V s^{-1}between −0.16 and 0.69 V vs Ag/Ag/Cl (thin line) after holding the potential at −0.16 V vs Ag/AgCl for 60 s (thick line). The arrow shows the time at which the potential scan begins. B: plot of the mass change associated with the gold oxide formation vs the Gibbs hydration energy of the cation.

41.1 ng cm^{-2}.

The observed mass increase attending gold oxidation ranged from 35.4 ng cm^{-2} for Li to 120 ng cm^{-2} for Cs, the mass increase monotonically decreasing with increasing hydration energy of the cation (Fig. 2B). Obviously, the adsorption of water and/or hydrated cations is largely responsible for the observed mass increase. Probably, the more hydrated a cation is, the more difficult will be its adsorption on the electrode.

3.1. Electrooxidation of 1-heptanol

3.1.1. Cycling voltammetry at 0.01 V s^{-1} in 10 mM 1-heptanol

The 1st and 2nd CVs (subsequent CVs showed no further changes) at 0.01 V s^{-1} in 0.1 M MOH in the presence of 10 mM heptanol, with heptanol admitted at open circuit, are shown in Fig. 3A and B, respectively. As already reported [4], the CVs show two anodic peaks of heptanol oxidation, one in the positive potential scan (peak *b1*) and the other one in the negative scan (peak *b2*). The charges in the positive scan were higher in the second scan (Fig. 3C), both when the alcohol was added at open circuit or at controlled potential. This result is in agreement with the recent study by Zhang et al. [14] of the oxidation of ethanol on gold in 0.1 M KOH, using in-situ liquid SIMS under operando conditions. They found that $Au(OH)_{ads}$ species were responsible for the oxidation of the alcohol, and that more $Au(OH)_{ads}$ species were available in the cathodic direction than in the anodic direction.

The onset potentials, taken to be as those at which the current density was 0.05 mA cm^{-2}, have been plotted as a function of the Gibbs hydration energy of the cation in Fig. 3D. Again, as in the absence of heptanol (Fig. 1B), no clear correlation can be established between the onset potentials and the Gibbs hydration energy.

3.1.2. Electrochemical Impedance Spectroscopy (EIS)

Since no clear trend of the influence of the cation on the activity of gold for the oxidation of 1-heptanol in 0.1 M hydroxide was observed in the CVs (Fig. 3), impedance measurements were carried 0.010 V vs Ag/AgCl, the onset potential for the oxidation of 1-heptanol, at which small differences in the onset potential in the different electrolytes would largely affect the measured charge-transfer resistance. Effectively, as shown below this was the case.

The Nyquist plots in the absence of 1-heptanol (Fig. 4) at 0.01 $V_{Ag/}$

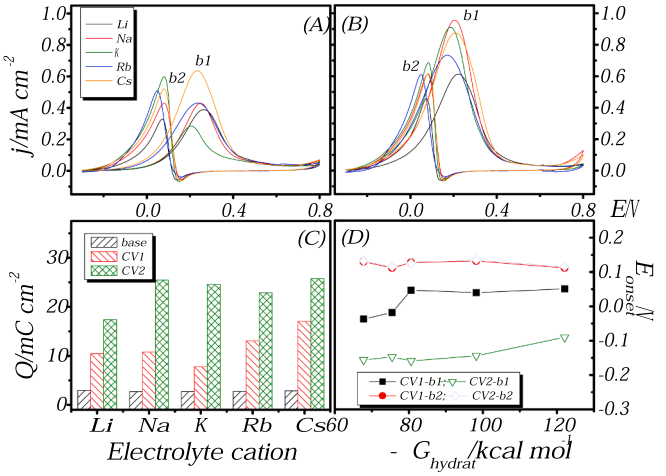

Fig. 3. 1st (A) and 2nd (B) consecutive cyclic voltammograms at 0.01 V s^{-1} of a gold disc electrode in 0.1 M MOH containing 10 mM 1-heptanol. The bar plot (C) shows the electrical charge of the positive potential scan in 0.1 M MOH (base), and in the 1st and 2nd CVs in the presence of 10 mM 1-heptanol. The plot labelled (D) shows the onset potentials for the oxidation peaks b1 and b2 of heptanol, taken to be as those at which the current density reached 0.05 mA cm^{-2} in CV1 and CV2.

$_{AgCl}$ were barely affected by the nature of the cation. They are typical of an R_u-C_{pseudo} series circuit, where R_u is the uncompensated electrolyte resistance and C_{pseudo} the pseudocapacitance of a non-ideal capacitor, known as a constant phase element. The fitted parameters, determined using the Fit and Simulation function of the Nova 2.1.1 software, are given in Table 1(a).

In the presence of 5 mM 1-heptanol, also at 0.01 V vs Ag/AgCl, the characteristic semicircle in the Nyquist plot is observed (Fig. 5), evidencing that heptanol oxidation takes place, in agreement with the CVs in Fig. 3A and B. As expected for measurements at the onset potential, at which the current is far lower than the diffusion-limited current, no Warburg resistance was observed. The data were fitted to a Randles equivalent circuit, $R_u(R_FC_{dl})$, namely, an uncompensated electrolyte resistance (R_u), in series with a faradaic resistance (R_F) in parallel with a double layer capacity (C_{dl}). The values of these parameters are given in Table 1(b). The faradaic resistance increased monotonically from LiOH to RbOH, its value for RbOH being about 4 times higher than that for LiOH, while the value for CsOH was the same as that for KOH. This result shows that EIS measurements at a fixed potential in the onset potential region can discriminate small differences in electrooxidation activity which are not clearly apparent in the onset potentials.

3.2. Probability of finding water molecules near the OH group of 1-heptanol in 0.1 M alkali metal hydroxides

The probability, *g(r)*, of finding water molecules at a given distance of the oxygen atom in the OH group of 1-heptanol in pure water and in 0.1 M solutions of different alkali metal cations, in the absence and the presence of a gold surface, is plotted in Fig. 6A and B, respectively. The results for hexanol have been already reported [4], the probabilities of finding water near the alcoholic OH group being higher than those for heptanol, as was to be expected due to the higher hydrophobicity of the latter. The probability, *g(0.2 nm)*, of finding water in the first hydration sphere of the OH group of heptanol (at about 0.2 nm from the oxygen atom) decreases dramatically in 0.1 M MOH as compared with its value in pure water (the probability at 1 nm was normalized to 1) (Fig. 6A). The probability in 0.1 M MOH decreased very strongly, and linearly, with increasing Gibbs hydration energy of the cation, from Cs^+ to Li^+,

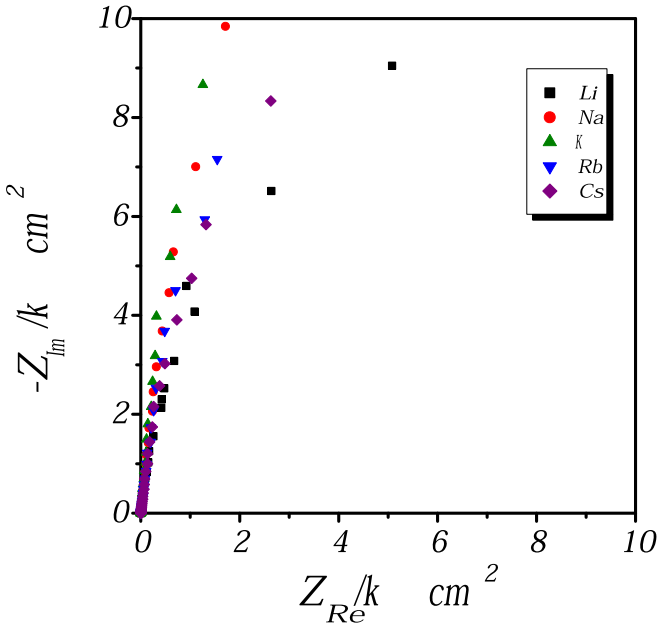

Fig. 4. Nyquist plots of a gold disc electrode in 0.1 M MOH at 0.010 V vs Ag/AgCl, with M = Li, Na, K, Rb and Cs.

Table 1
EIS parameters at 0.010 V vs Ag/AgCl of a gold disc in 0.1 M MOH solutions (a) and in 0.1 M MOH solutions containing 5 mM 1-heptanol (b) (from Nyquist plots in Figs. 4 and 5, respectively).

MOH	0.1 M MOH (a)		5 mM 1-heptanol in 0.1 M MOH (b)		
	R_u/Ω cm^2	C_{pseudo}/μF cm^{-2}	R_u/Ω cm^2	R_F/kΩ cm^2	C_{dl}/μF cm^{-2}
LiOH	4.7	309	7.6	3.7	38.1
NaOH	3.8	290	8.5	6.0	21.2
KOH	5.0	249	8.1	10.6	35.8
RbOH	6.9	281	6.2	16.7	22.9
CsOH	6.3	287	4.9	10.3	34.2

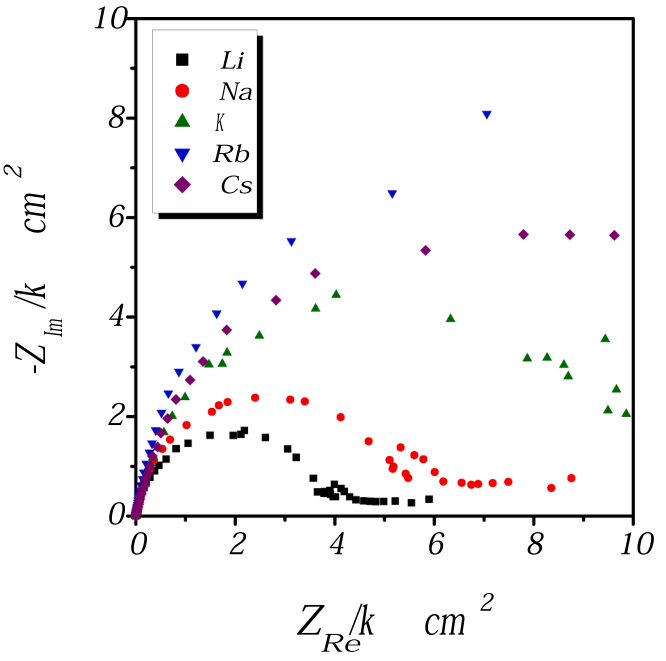

Fig. 5. Nyquist plots at 0.010 V vs Ag/AgCl of a gold disc electrode in 0.1 M MOH +5 mM 1-heptanol, with M = Li, Na, K, Rb and Cs.

and was only slightly affected by the presence of the gold surface (Fig. 7).

Since the charge-transfer resistance for the oxidation of 1-heptanol increased monotonically from LiOH to RbOH, its value for RbOH being about 4 times higher than that for LiOH, that is, the heptanol oxidation current at a fixed potential decreased from LiOH to RbOH, it can be concluded that a smaller hydration of the heptanol OH group favours its access to the gold surface. The only exception is CsOH, for which the charge-transfer resistance was the same as that with KOH.

4. Conclusions

As already reported [4], the oxidazability of linear saturated aliphatic alcohols from C1 to C7 on gold in alkali metal hydroxides increased with increasing chain length, that is, with decreasing hydration of the alcohol, as confirmed by molecular dynamics simulation. This decreasing hydration would facilitate the access of the alcohol to the electrode surface. Here we have found a similar result, namely, that the charge-transfer resistance at a fixed potential of 1-heptanol oxidation on gold in 0.1 M MOH electrolytes increased by a factor of 4 from LiOH to RbOH, that is, the heptanol oxidation current decreased. Since the degree of hydration of the OH group of the alcohol, as estimated by Molecular Dynamics Simulation, increased by a factor of 5 from LiOH to RbOH, the simplest explanation possible is that the decrease of the heptanol oxidation current from LiOH to RbOH is due to an increasing

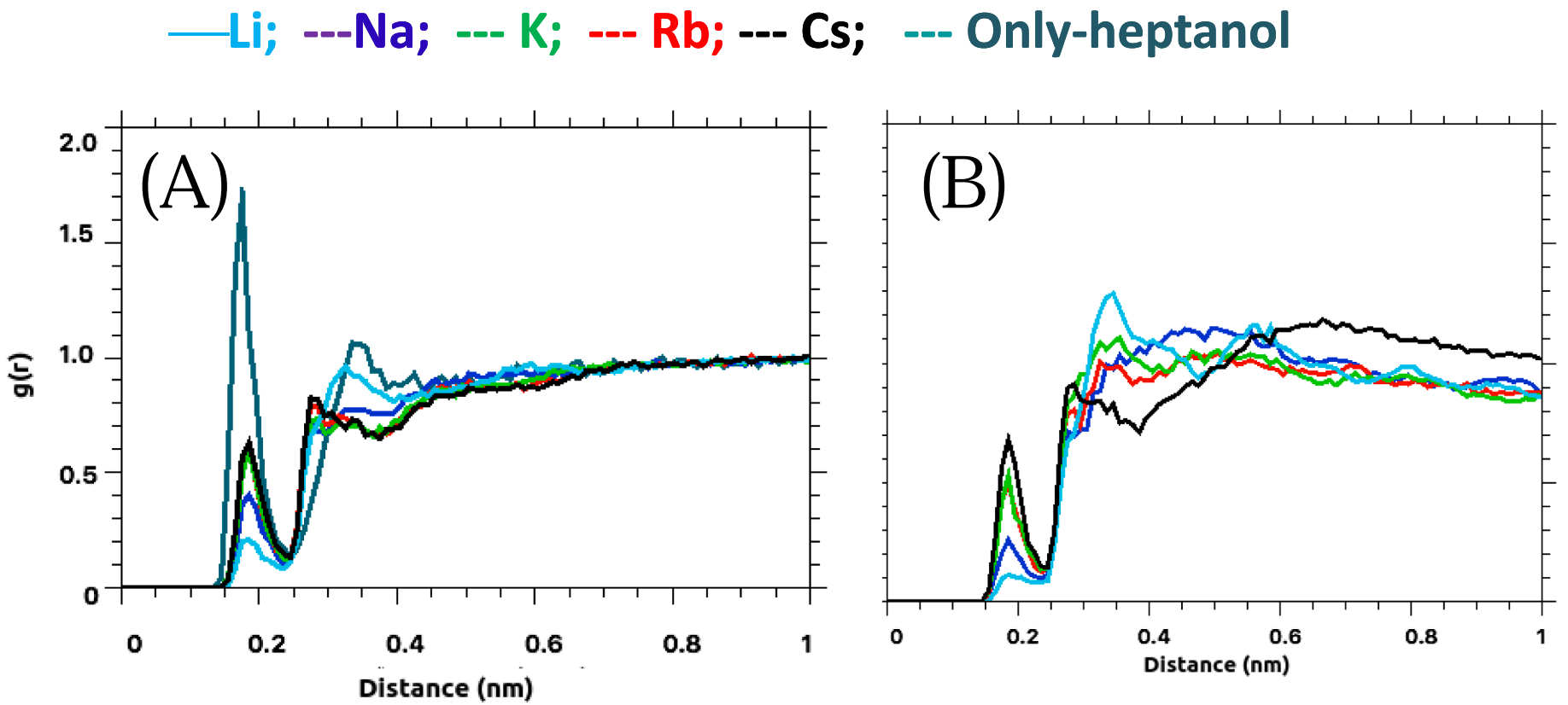

Fig. 6. Probability, g(r), obtained by Molecular Dynamics Simulation, of finding water molecules as a function of the distance, r, of the oxygen atom in the OH group of 1-heptanol, in water and in 0.1 M solutions of different alkali metal hydroxides, in the absence (Fig.6A) and the presence (Fig.6B) of a gold surface. The sharp maxima at about 0.2 nm correspond to the inner hydration sphere of the OH group of 1-heptanol.

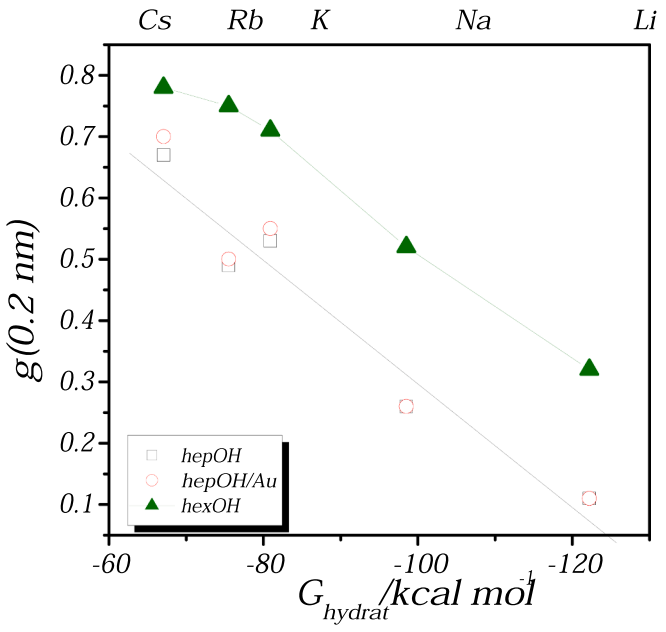

Fig. 7. Dependence on the Gibbs energy hydration of the alkali metal cations of the probability of finding water in the inner hydration sphere of the OH group of the alcohol (value of g(r) at about 0.2 nm of the oxygen atom in the OH group) in different 0.1 M alkali metal hydroxides. Squares: 1-heptanol; circles: 1-heptanol in the presence of an Au(111) gold surface; triangles: 1-hexanol.

hydration of the heptanol OH group, which would hinder its access to the electrode surface. Although the EIS measurement in CsOH did not fit this trend, we think that the nature of the cation in the alkali metal hydroxide significantly affects the electrooxidation of 1-heptanol on gold, in a clear case of non-covalent interaction.

Declaration of competing interest

None.

CRediT authorship contribution statement

M. Soledad Ureta-Zañartu: Funding acquisition, Writing - original draft. **Ana María Méndez-Torres:** Data curation. **Francisco Fernández:** Investigation, Data curation. **Jacqueline Ilabaca:** Investigation, Data curation. **Carolina Mascayano:** Formal analysis. **Claudio Gutiérrez:** Writing - original draft.

Acknowledgements

This work was supported by Fondo Nacional de Ciencia y Tecnología (FONDECYT-CONICYT-Chile), under Grants 1140207 and 1120379 and by Universidad de Santiago de Chile (USACh), Vicerrectoría de Investigación, Desarrollo e Innovación (VRIDEI)-Grant USA 1899, 021941UZ-PAP and Dirección de Investigación en Ciencia y Tecnología (DICYT)-USACh 021841UZ.

References

[1] D. Strmcnik, K. Kodama, D. Van der Vliet, J. Greeley, V.R. Stamenkovic, N. M. Marković, Nat. Chem. 1 (2009) 466–472.
[2] M. Nakamura, Y. Nakajima, K. Kato, O. Sakata, N. Hoshi, J. Phys. Chem. C 119 (2015) 23586–23591.
[3] R. RAdžić, M. Avramov-Ivić, J. Catal. 101 (1986) 532–535.
[4] M.S. Ureta-Zañartu, C. Mascayano, C. Gutiérrez, Electrochim. Acta 165 (2015) 232–238.
[5] P. Chulkin, M. Lapkowski, M.R. Bryce, J. Santos, P Data, Electrochim Acta 258 (2017) 1160–1172.
[6] S. Trasatti, O. Petrii, Pure Appl. Chem. 63 (1991) 711–734.
[7] Gaussian 03, Revision A.1 M.J. Frisch, G.W. Trucks, H.B. Schlegel, G.E. Scuseria, M.A. Robb, JR. Cheeseman, G. Scalmani, V. Barone, B. Mennucci, G.A. Petersson, H. Nakatsuji, M. Caricato, X. Li, H.P. Hratchian, A.F. Izmaylov, J. Bloino, G. Zheng, J.L. Sonnenberg, M. Hada, M. Ehara, K. Toyota, R. Fukuda, J. Hasegawa, M. Ishida, T. Nakajima, Y. Honda, O. Kitao, H. Nakai, T. Vreven, J.A. Montgomery Jr., J. E. Peralta, F. Ogliaro, M. Bearpark, J.J. Heyd, E. Brothers, K.N. Kudin, V. N. Staroverov, R. Kobayashi, J. Normand, K. Raghavachari, A. Rendell, J.C. Burant, S.S. Iyengar, J. Tomasi, M. Cossi, N. Rega, J.M. Millam, M. Klene, J.E. Knox, J. B. Cross, V. Bakken, C. Adamo, J. Jaramillo, R. Gomperts, R.E. Stratmann, O. Yazyev, A.J. Austin, R. Cammi, C. Pomelli, J.W. Ochterski, R.L. Martin, K. Morokuma, V.G. Zakrzewski, G.A. Voth, P. Salvador, J.J. Dannenberg, S. Dapprich, A.D. Daniels, Ö. Farkas, J.B. Foresman, J.V. Ortiz, J. Cioslowski, D. J. Fox, Gaussian, Inc., Wallingford CT, 2009.
[8] E.F. Pettersen, T.D. Goddard, C.C. Huang, G.S. Couch, D.M. Greenblatt, E.C. Meng, T.E. Ferrin, J. Comput. Chem. 25 (2004) 1605–1612.
[9] L. Kalé, R. Skee, M. Bhandarkar, R. Brunner, A. Gursoy, N. Krawetz, J. Phillips, A. Shinozaki, K. Varadarajan, K. Schulten, J. Comput. Phys. 151 (1999) 283–382.
[10] B.R. Brooks, R.E. Bruccoleri, B.D. Olafson, D.J. States, S. Swaminathan, M. Karplus, J. Comput. Chem. 4 (1983) 187–217.
[11] W. Humphrey, A. Dalke, K. Schulten, J. Mol. Graph. 14 (1996) 33–38.
[12] J. Wang, W. Wang, P.A. Kollman, DA case, J. Mol. Graph. Model. 25 (2006) 247–260.
[13] J. Aqvist, J. Phys. Chem. 94 (1990) 8021–8024.
[14] Y. Zhang, J.-G. Wang, X. Yu, D.R. Baer, Y. Zhao, L. Mao, F. Wang, Z. Zhu, ACS Energy Lett 4 (2019) 215–221.